EUROPEAN ORGANIZATION FOR PARTICLE PHYSICS

CERN–PPE/94–85
31 May 1994

Inclusive measurement of $\bar{p}$ annihilation at rest in gaseous hydrogen to final states containing ρ and f_2

The CPLEAR Collaboration

R. Adler[2], T. Alhalel[11], A. Angelopoulos[1], A. Apostolakis[1], E. Aslanides[4,11], G. Backenstoss[2], C.P. Bee[4], O. Behnke[17], J. Bennet[9], V. Bertin[11,a], J.K. Bienlein[17,b] P. Bloch[4], Ch. Bula[13,c], P. Carlson[15], J. Carvalho[5], E. Cawley[9], S. Charalambous[16], M. Chardalas[16], G. Chardin[14], M.B. Chertok[3], M. Danielsson[15], A. Cody[9,d], S. Dedoussis[16], M. Dejardin[4], J. Derre[14], M. Dodgson[9,e], J.C. Dousse[7] J. Duclos[14], A. Ealet[11], B. Eckart[2], C. Eleftheriadis[16], I. Evangelou[8], L. Faravel[7], P. Fassnacht[11], J.L. Faure[14], C. Felder[2], R. Ferreira-Marques[5], W. Fetscher[17], M. Fidecaro[4], A. Filipčič[10], D. Francis[3], J. Fry[9], C. Fuglesang[15,f], E. Gabathuler[9], R. Gamet[9], D. Garreta[14], T. Geralis[13,a], H.-J. Gerber[17], A. Go[3], P. Gumplinger[17,g], C. Guyot[14], P.F. Harrison[9,h], A. Haselden[9], P.J. Hayman[9], F. Henry-Couannier[11], W.G. Heyes[4,i], R.W. Hollander[6], K. Jansson[15], H.U. Johner[7,j], K. Jon-And[15], A. Kerek[15], J. Kern[7], P.R. Kettle[13], C. Kochowski[14], P. Kokkas[8], R. Kreuger[6], T. Lawry[3,k], R. Le Gac[11], A. Liolios[16], E. Machado[5], P. Maley[9], I. Mandić[10], N. Manthos[8], G. Marel[14], M. Mikuž[10], J. Miller[3], F. Montanet[11], T. Nakada[13], A. Onofre[5], B. Pagels[17], P. Pavlopoulos[2], F. Pelucchi[11,l], J. Pinto da Cunha[5], A. Policarpo[5], G. Polivka[2], H. Postma[6], R. Rickenbach[2], B.L. Roberts[3], E. Rozaki[1], T. Ruf[4], L. Sacks[9,m], L. Sakeliou[1], P. Sanders[9], C. Santoni[2], K. Sarigiannis[1], M. Schäfer[17], L.A. Schaller[7], A. Schopper[4], P. Schune[14], A. Soares[14], L. Tauscher[2], C. Thibault[12], F. Touchard[4,11], C. Touramanis[16], F. Triantis[8], D.A. Tröster[2,n], E. Van Beveren[5], C.W.E. Van Eijk[6], G. Varner[3], S. Vlachos[9], P. Weber[17], O. Wigger[13], C. Witzig[17,o], M. Wolter[17], C. Yeche[14], D. Zavrtanik[10] and D. Zimmerman[3].

Abstract

Antiproton annihilation at rest in gaseous hydrogen (16 bar pressure) to the final states $\rho(770)X$ and $f_2(1270)X$, where X stands for one or more neutral mesons, has been studied at LEAR using the CPLEAR detector. Relative branching ratios are given for $X = \pi^0, 2\pi^0, 3\pi^0, \omega$ in the ρ case, and for $X = \pi^0, \eta$ in the f_2 case. The annihilation channel $\bar{p}p \to \rho 3\pi^0$ has not been measured before. The fraction of P-wave annihilation is deduced from the ratio $f_2\pi^0/\rho\pi^0$ to be 0.38 ± 0.07, in good agreement with the result previously obtained by CPLEAR from the ratio $K^+K^-/\pi^+\pi^-$.

(To be submitted to Zeitschrift f. Physik C)

[1]University of Athens, GR-10680 Athens, Greece
[2]University of Basle, CH-4056 Basle, Switzerland
[3]Boston University, Boston, MA 02215, USA
[4]CERN, CH-1211 Geneva 23, Switzerland
[5]LIP and University of Coimbra, P-3000 Coimbra, Portugal
[6]Delft University of Technology, 2629 JB Delft, Netherlands
[7]University of Fribourg, CH-1700 Fribourg, Switzerland
[8]University of Ioannina, GR-45110 Ioannina, Greece
[9]University of Liverpool, Liverpool L69 3BX, UK
[10]J. Stefan Inst. and Phys. Dep., University of Ljubljana, SI-61111 Ljubljana, Slovenia
[11]CPPM, IN2P3-CNRS et Université d'Aix-Marseille II, F-13288 Marseille, France
[12]CSNSM, IN2P3-CNRS, F-91405 Orsay, France
[13]Paul-Scherrer-Institut(PSI), CH-5232 Villigen-PSI, Switzerland
[14]DAPNIA/SPP, CE Saclay, F-91191 Gif-sur-Yvette, France
[15]Royal Institute of Technology, S-10405 Stockholm, Sweden
[16]University of Thessaloniki, GR-54006 Thessaloniki, Greece
[17]ETH-ITP Zürich, CH-8093 Zürich, Switzerland
[a]Now at RAL, Didcot, UK
[b]Permanent address: DESY, Hamburg, Germany
[c]Now at Princeton University, Princeton, NJ, USA
[d]Visitor from University College, Dublin, Ireland
[e]Now at CERN, Switzerland
[f]Now at ESA/EAC, Köln, Germany
[g]Now at TRIUMF, Vancouver, Canada
[h]Now at QMW, University of London, UK
[i]Now at CEBAF, Newport News, VA, USA
[j]Now at SUeR, Fribourg University, Switzerland
[k]Now at University of Virginia, Charlottesville, VA, USA
[l]Now at INFN, Frascati, Italy
[m]Now at UCL, University College, London, UK
[n]Now at SBS, Basle, Switzerland
[o]Now at Brookhaven National Laboratory, Upton, NY, USA

1 Introduction

The $\bar{\mathrm{p}}\mathrm{p}$ annihilation at rest is still far from being fully understood. This remains so despite the large amount of data being accumulated by bubble chambers, and more recently by dedicated spectrometers like ASTERIX [1], Crystal Barrel [2], and OBELIX [3] which were built around the Low-Energy Antiproton Ring (LEAR) at CERN. The experimental situation is summarized in the review articles by Armenteros and French [4], and by Amsler and Myhrer [5].

The CPLEAR experiment [6], is designed to study the discrete symmetries (CP, T, CPT) in the neutral kaon system. Our inclusive measurements of $\bar{\mathrm{p}}\mathrm{p}$ annihilation taken for calibration purposes provide useful information about some of the annihilation channels. Here we will report on the relative branching ratios of $(\pi^+\pi^-)$ resonances, ρ and f_2, associated with one or more neutral mesons (π^0, ω, η). With our target pressure of 16 bar, the atomic cascade of $\bar{\mathrm{p}}$ leads to a ratio of S- and P-wave annihilation which falls between previous measurements with either liquid hydrogen or low-pressure (≤ 1 bar) hydrogen gas targets. One of the final states (ρ^0 accompanied by three π^0's) was isolated for the first time.

In Section 2, we describe briefly the CPLEAR spectrometer and the data selection. In Section 3, we discuss the data analysis and present the relative branching ratio results. The fraction of P-wave annihilation in a 16 bar hydrogen gas target is determined in Section 4.

2 Experiment and data

The detector has a cylindrical shape and is contained within a solenoid of 3.6 m length and 2 m diameter, providing a magnetic field of 0.44 T. Antiprotons were provided by LEAR with a momentum of 200 MeV/c, and monitored by a scintillator counter in front of the target. They stop and annihilate at a rate of ≈ 1 MHz at the centre of the detector in a spherical target of 14 cm diameter filled with gaseous hydrogen at 16 bar. Two proportional chambers, six drift chambers, and two layers of streamer tubes perform the tracking of charged particles within a cylinder of ≈ 60 cm radius. Outside the tracking devices, there is a particle identification detector consisting of a layer of Cherenkov counters sandwiched by scintillators S_1 and S_2, and a high-granularity gas-sampling electromagnetic calorimeter.

The data reported here are part of the data collected in 1990, and were taken with a minimum bias trigger (requiring at least one hit in the scintillator S_1 in coincidence with the incoming antiproton) which was otherwise used for calibration purposes. The sample contains 3.1 M events, well balanced between opposite magnetic field polarity settings. The calorimeter was not fully operational during this period and thus was not used for the following analysis.

For this work we analysed only events containing two tracks, i.e 30.8% of the total, which reduced to 13.8% after requiring that the following criteria were satisfied:

- the two tracks had opposite charges.
- at least two z and four (r, ϕ) coordinates per track were recorded. This leads to a momentum resolution of $\Delta p/p \cong (0.05^2 + (0.1 \times p)^2)^{1/2}$, ($p$ in GeV/c).

- the vertex was found within the annihilation region defined as a cylinder of 1.5 cm radius and 10 cm length.

All particles were assumed to be pions since charged particle emission other than pions is very scarce in $\bar{p}p$ annihilation at rest.

For the remaining events, the invariant mass $m_{\pi\pi}$ is calculated from the two tracks. The resolution is found by Monte Carlo (MC) simulation to be $\sigma(m_{\pi\pi}) \approx 35$ MeV/c^2 at 770 MeV/c^2, and ≈ 70 MeV/c^2 at 1270 MeV/c^2, depending slightly on the phase space of the annihilation channel. The invariant mass spectrum is shown in Fig. 1 and forms the basis of the analysis described in the following sections. The drop-off at low mass (below 450 MeV/c^2) is caused by our detector acceptance (minimal momentum required to reach the scintillator S_1). The end-point at the high masses is given by the phase space of the $\bar{p}p$ system. Three resonances show up on top of a steep and exponential-like background of non-resonant two-track events. The resonances are identified as the $\rho(770)$, the $f_2(1270)$, and the $a_X(1565)$. However, since the final states containing a_X are limited by phase space, we shall study only final states associated with ρ- and f_2-production.

3 Analysis of data

3.1 The invariant mass spectrum

To analyse the invariant mass spectrum of Fig. 1, a simultaneous fit of the three resonances plus the non-resonant background was performed. The shape of each resonance used in the fit was obtained by MC simulation. A Breit-Wigner distribution was used for the mass of the resonances (central value and width according to [7] for ρ and f_2, and to [8] for a_X). For all final states known to consist of either ρ or f_2 plus neutral mesons, and for $a_X\pi^0$, events were generated from the corresponding phase space. The events were tracked through the detector using a GEANT3 [9] simulation code, and subsequently subjected to the same off-line analysis as real data. While the resulting invariant mass spectrum of ρ was found to be largely independent of the final states, the shape of f_2 was affected by the amount of $f_2\eta$ because of its limited phase space. Each resonance was given only one overall weight factor (free parameter in the fit) with respect to the background. Among the various background parametrizations (exponential, polynomial, power functions), the best χ^2 is found for the power function suggested in Ref. [10], $F(m) = (p_5 - m)^{p_1} e^{p_2} + (p_5 - m)^{p_3} e^{p_4}$, where $m \equiv m_{\pi\pi}$ is the invariant mass, and p_1 to p_5 are fit parameters.

The fit to the invariant mass spectrum was obtained through reiteration. The relative branching ratios for final states containing f_2, determined by analysing the momentum spectrum (see Section 3.2), were implemented in the simulation as feed-back for an improved determination of the f_2 resonance shape. The invariant mass spectrum was fitted again, thus giving a better description of f_2. The result of this fit provided the starting values for the final fit. In the latter, the Breit-Wigner distributions and the background, parametrized as mentioned above, were fitted to the data, keeping free the central values M_{ρ,f_2,a_X}, the widths Γ_{ρ,f_2,a_X}, and the relative weights of the resonances, as well as the background parameters.

To estimate the number of events in the peaks, the area under the fitted Breit-Wigner limited in the range $M_{\rho,f_2} \pm \frac{1}{2}\Gamma_{\rho,f_2}$ was used, giving 36400$\pm$900 events for the ρ and 7240$\pm$600 events for the f_2. The error in the number of events is dominated by the uncertainty of the background parametrization. In all our attempts to fit the invariant mass spectrum, the result was improved by including the a_X. In the course of our full analysis, however, we found that the inclusion or discarding of this resonance did not have any significant impact on the branching ratio results for the ρ- and f_2- annihilation channels.

The final result of the fit to the invariant mass spectrum is shown by the full line in Fig. 1 (χ^2/NDF = 103/50). The background is drawn separately as a dashed line. The background-subtracted invariant mass spectrum is displayed in Fig. 2, where the full line is the sum of the three Breit-Wigner distributions given by the fit to the spectrum of Fig. 1. The f_2 peak is shifted to a slightly lower mass compared to the tabulated [7] value, because of the limited phase space of $f_2\eta$. This is well reproduced by the MC-generated invariant mass spectrum for the amount of $f_2\eta$ found in our analysis.

3.2 The momentum spectrum

The analysis to determine the branching ratios of annihilation channels with ρ and f_2 production was based on the momentum spectrum obtained with the resonant events in the slice $M_{\rho,f_2} \pm \frac{1}{2}\Gamma_{\rho,f_2}$ (see Fig. 1). In order to estimate the background shape from the large number of non-resonant events present in the two regions, additional slices (100 MeV/c^2 wide) were selected on each side. The slices are drawn in Fig. 1 as dotted and dashed-dotted lines for ρ and f_2 respectively. The momentum spectrum of the ρ events (f_2 events) is displayed in Fig. 3 (Fig. 5). The momentum spectrum of the events in the low-mass (high-mass) background slice is drawn as a dashed (dotted) line for both the ρ and f_2 in Figs. 3 and 5 respectively.

To unfold the ρ and f_2 momentum spectrum, MC-generated momentum spectra for the final states containing ρ and f_2 were produced from the event simulation described above for the invariant mass fit. The shape characteristic for the different channels as well as the acceptance were obtained. Each channel was given an overall weight (free parameter in the fit) in order to determine the relative branching ratios in the fit of the momentum spectrum.

The background-subtracted invariant mass spectrum of Fig. 2 reveals that the ρ peak extends under the f_2 peak and vice versa. Moreover, resonant events also populate the background slices. Both effects were studied by MC simulations in order to take the background properly into account in the ρ and f_2 momentum distributions. The input distributions for fitting the momentum spectrum of Figs. 3 and 5 were given by:
1) the MC-generated shape of the various annihilation channels with ρ and f_2;
2) the measured momentum spectrum of the background slices on each side of ρ and f_2;
3) the MC-generated shape of resonant events in the background, and of resonant events from the neighbouring resonance.

The relative contribution of the various annihilation channels and the weights of the background, corrected for the resonant events, were fitted simultaneously for the momentum spectrum of ρ and f_2. Consistency of the fit is demanded by the constraint imposed on the results of the invariant mass fit, i.e. the number of resonant and background events.

The total background (lower solid line in Figs. 3 and 5) is the weighted sum of the two background contributions. The weight factors, 0.69$\pm$0.09 (0.70$\pm$0.03) for the low-mass background slice, and 0.80$\pm$0.17 (1.22$\pm$0.08) for the high-mass background slice of the ρ (f_2) momentum spectrum, correspond to the best fit of the data in Fig. 3 (Fig. 5).

From a previous analysis of multi-pion final states in $\bar{\rm p}$p annihilations [11] we expect $\rho 4\pi^0$ to be much less frequent than $\rho 3\pi^0$. We have therefore excluded channels with four or more π^0s from our analysis.

The ρ momentum spectrum:
We have concentrated our analysis on the channels $\rho\pi^0$, $\rho\pi^0\pi^0$, $\rho\pi^0\pi^0\pi^0$, and $\rho\omega$. As it was not possible to sufficiently separate the $\rho\eta$ and $\rho\pi^0\pi^0$ channels, we adopted a world average value of 0.312±0.074 for the $\rho\eta/\rho\pi^0$ relative branching ratio [1] . The amount of events in the channels $\rho\pi^0$, $\rho\pi^0\pi^0$, $\rho\pi^0\pi^0\pi^0$, and $\rho\omega$ is obtained by a least squares fit to the data of Fig. 3 using the momentum distributions obtained from the simulation for all these channels and the momentum spectrum of the background. The world average of the ratio $\rho\eta/\rho\pi^0$ and the number of events in the ρ peak (36400) were used as constraints, and the weights of the individual channels were fitted. The best fit gives a χ^2 of 48 for 45 degrees of freedom, the result of which is shown in Fig. 3. The background-subtracted momentum spectrum of ρ is displayed in Fig. 4, together with the individual contributions of $\rho\pi^0$, $\rho\eta$, $\rho\pi^0\pi^0$, $\rho\pi^0\pi^0\pi^0$, and $\rho\omega$. If $\rho\pi^0\pi^0\pi^0$ is omitted in the analysis, the fit to the momentum spectrum fails to reproduce the number of ρ events, and the χ^2 is increased to 132. We conclude that this channel is present in $\bar{\rm p}$p annihilations.

The numbers of events found for the individual channels are listed in Table 1. The acceptance-corrected numbers of events are given with statistical and systematic errors to be used for the calculation of the branching ratios. Note that the acceptance for $\rho\omega$ is an order of magnitude smaller than the others, because of the small decay branching ratio of $\omega(\rightarrow \text{neutral}) = 8.5\%$. The systematic errors in Table 1 result from:
1) uncertainties in the background parametrization of the invariant mass spectrum. The error was estimated by variation of the background parametrization, i.e. varying the weight, position, and width of the background slices, as well as trying different analytical functions for the fit to the background in the invariant mass spectrum. Background parametrization leads to the largest contribution of systematic errors.
2) uncertainties in the shape of the MC-generated distributions. Errors arising from the MC simulation of the different channels have been estimated by modifying the input parameters to the MC (detector resolution, mass and width of the resonances, and relative branching ratios of intermediate resonant as well as final states).
3) uncertainties from the relative branching ratio $\rho\eta/\rho\pi^0$ which was fixed in the fit to 0.312. The fit was repeated with values varying within ±0.074 and the change in results determined the systematic error. The fit was also done leaving both $\rho\eta$ and $\rho\pi^0$ free, which gave a solution with no $\rho\pi^0\pi^0$ contribution. Such a result seems very unlikely.
4) uncertainties from background channels. The annihilation channels $\bar{\rm p}{\rm p} \rightarrow \rho\pi^+\pi^-$ and $\bar{\rm p}{\rm p} \rightarrow \rho\pi^0\pi^+\pi^-$ both have high branching ratios [12]. We have studied the acceptance for the case where the detector misses the two non-resonant charged pions. Our MC simulations show that only a few events of this type pass our analysis requirements and hence do not affect the branching ratios for ρ plus neutral meson production much.

[1] The world average value of 0.312±0.074 for the relative branching ratio of $\rho\eta/\rho\pi^0$ was obtained from experiments using either liquid hydrogen [12, 13, 14, 15] or gaseous hydrogen at NTP [16, 17]. The results of Refs. [16, 17] suggest that the relative branching ratio $\rho\eta/\rho\pi^0$ varies very little from pure S-wave to pure P-wave annihilation. Note that the error on $\rho\eta$ is much larger than on $\rho\pi^0$.

Channel	Events	Acceptance	Acceptance-corrected events
$\rho\pi^0$	12750	17.3%	73700 $\pm$3100 $\pm$1200
$\rho\pi^0\pi^0$	4910	16.2%	30000 $\pm$13000 $\pm$6000
$\rho\pi^0\pi^0\pi^0$	12580	15.3%	82200 $\pm$8800 $\pm$10000
$\rho\omega$	3200	1.62%	196700 $\pm$30900 $\pm$8000
$f_2\pi^0$	5710	9.35%	61100 $\pm$3000 $\pm$1000
$f_2\eta$	1650	7.35%	22500 $\pm$3000 $\pm$10000

Table 1: *Number of events before and after acceptance correction. Statistical and systematic errors are given for the acceptance-corrected event numbers. The acceptance includes the branching ratio of $\omega, \eta(\to$ neutrals). (The relative branching ratio $\rho\eta/\rho\pi^0$ was fixed to the value 0.312.)*

The f_2 momentum spectrum:
We have limited our analysis to the channels $f_2\pi^0$ and $f_2\eta$. The analysis proceeds analogously to the one for the ρ channels. The f_2 momentum spectrum is displayed in Fig. 5 together with the contributions from the background slices. The background-subtracted momentum spectrum of f_2 is given in Fig. 6. The $f_2\pi^0$ and $f_2\eta$ channels are well separated. The number of f_2 events (7200 ± 600) obtained from the invariant mass spectrum was used as the only constraint to the fit of the momentum spectrum. The best fit in Fig. 6 gives a χ^2/NDF = 64/47. The number of events for the $f_2\pi^0$ and $f_2\eta$ channels are listed in Table 1. The acceptance correction takes into account the decay branching ratio of $\eta(\to$ neutral) = 70.8%. The quality of the fit to the f_2 momentum spectrum is fine except for momenta < 200 MeV/c. In this low-momentum region, the annihilation channels $f_2\pi^0\pi^0$ and $f_2\pi^0\pi^0\pi^0$ possibly contribute to the spectrum. If both $f_2\pi^0\pi^0$ and $f_2\pi^0\pi^0\pi^0$ are included in the analysis, the χ^2 does not get worse, but the result of the fit seems unlikely with no events for $f_2\pi^0\pi^0$, whilst $f_2\pi^0\pi^0\pi^0$ becomes relatively important at half the strength of $f_2\eta$.

3.3 Relative branching ratios

Our results for the relative branching ratios $\rho\pi^0\pi^0/\rho\pi^0$, $\rho\pi^0\pi^0\pi^0/\rho\pi^0$, $\rho\omega/\rho\pi^0$, and $f_2\pi^0/\rho\pi^0$ and $f_2\eta/f_2\pi^0$ are given in Table 2. The errors are obtained by quadratically adding the statistical and systematic errors of Table 1.

Earlier results from annihilation in liquid hydrogen (with $\approx 10-20\%$ P-wave annihilation, c.f. Section 4) and more recent data from the ASTERIX experiment [16, 17, 19], where results were extrapolated to pure S- and P-wave annihilation, are listed in Table 2. Direct comparison of measurements in liquid and gaseous hydrogen targets is not straightforward, since the branching ratios generally depend on the amount of P-wave annihilation (see ASTERIX results).

For $\rho + n\pi^0$, ($n \geq 2$), only a small amount of information is available so far. There is one earlier result for $\rho\pi^0\pi^0$ with (1.37$\pm$0.24)% [18], whereas the $\rho\pi^0\pi^0\pi^0$ channel has not been

Branching ratio	This experiment	Pure S-wave (ASTERIX)	Pure P-wave (ASTERIX)	Liquid H_2
$\rho\pi^0\pi^0/\rho\pi^0$	0.41±0.20	-	-	0.87±0.16 [12, 13, 18]
$\rho\pi^0\pi^0\pi^0/\rho\pi^0$	1.12±0.19	-	-	-
$\rho\omega/\rho\pi^0$	2.67±0.45	1.89±0.53 [19]	15.9±4.6 [19]	1.20±0.44 [12, 13, 20]
$f_2\pi^0/\rho\pi^0$	0.83±0.06	0.25±0.08 [16]	4.6±1.2 [16]	0.27±0.08 [12, 13]
$f_2\eta/f_2\pi^0$	0.37±0.16	0.04±0.04 [16, 17]	0.06±0.03 [16, 17]	-

Table 2: *Relative branching ratios of $p\bar{p}$-annihilation. Results from this experiment are compared with values obtained for pure S- and P-wave annihilation, and annihilation in liquid hydrogen. The errors of our values include both statistical and systematic errors.*

measured before.

Comparison of the $f_2\eta$ channel with previous branching ratios [16, 17] is difficult because of the large errors.

4 Determination of the fraction of P-wave annihilation

The branching ratios of many final states strongly depend on the $\bar{p}p$ atomic state from which annihilation takes place. This effect has been demonstrated by the ASTERIX collaboration, who measured pure S- and P-wave annihilation using associated X-ray selection. On the other hand, it is well known that the atomic cascade of $\bar{p}$ depends on the density of the target material because of Stark mixing [21] , resulting in a density-dependent amount of S- and P-wave annihilation.

In liquid hydrogen, the fraction of P-wave annihilation, f_P, was estimated to be (18±2)% [22], in disagreement with Ref. [23] where a value of (28.8±3.5)% was found, and Ref. [16] with (8.6±1.1)% P-wave. Reifenröther and Klempt have calculated f_P to be $\approx$ 10% for liquid hydrogen, and $20-30\%$ for gaseous hydrogen at 16 bar, basically depending on the value assumed for the Auger rate [24].

Our result $R = 0.83 \pm 0.06$ for the relative branching ratio of $f_2\pi^0/\rho\pi^0$ permits the calculation of f_P at a hydrogen target pressure of 16 bar. The calculation of f_P requires the knowledge of the absolute branching ratios for pure S- and P-wave annihilation for both $f_2\pi^0$ and $\rho\pi^0$. Assuming the annihilation is restricted to S- and P-waves only, f_P is given by the relation:

$$f_P = \frac{\Gamma_S(f_2\pi^0) - R\Gamma_S(\rho\pi^0)}{R[\Gamma_P(\rho\pi^0) - \Gamma_S(\rho\pi^0)] - [\Gamma_P(f_2\pi^0) - \Gamma_S(f_2\pi^0)]} \quad .$$

The experimental values for the absolute branching ratios are taken from the ASTERIX collaboration, which for convenience are listed in Table 3 (the errors in different channels are uncorrelated [26]). Our result for the fraction of P-wave annihilation then becomes:

$$f_P(f_2\pi^0/\rho\pi^0) = 0.376{\pm}0.026_{internal}{\pm}0.065_{external} = 0.38{\pm}0.07_{total},$$

Channel	Γ_S (ASTERIX)	Γ_P (ASTERIX)	Ratio (this work)	f_P (16 bar) (This work)
$f_2\pi^0$	0.39±0.11%	1.83±0.23% [16]	$f_2\pi^0/\rho\pi^0$=0.83±0.06	0.38±0.07
$\rho\pi^0$	1.56±0.21%	0.40±0.09% [16]	$\rho\omega/\rho\pi^0$=2.67±0.45	0.19±0.15
$\rho\omega$	2.95±0.72%	6.35±1.14% [25]		

Table 3: *Fraction of P-wave annihilation, f_P, in gaseous hydrogen at 16 bar deduced from the relative branching ratios determined in this work. The absolute branching ratios for pure S- and P-wave annihilation are taken from the ASTERIX collaboration.*

where the internal error is the quadratic sum of our statistical and systematic errors. The external error comes from the uncertainties in the absolute branching ratios measured by ASTERIX and exceeds the internal error. The total error is the quadratic sum of both internal and external errors. This result is in agreement with our previous measurement of $f_P = 0.379 \pm 0.086$ [27] obtained for the relative branching ratio of the channels K^+K^- and $\pi^+\pi^-$ at the same target pressure of 16 bar.

Similarly, we evaluated the fraction of P-wave annihilation for the relative branching ratio $R(\rho\omega/\rho\pi^0) = 2.67 \pm 0.45$, and obtained:

$$f_P(\rho\omega/\rho\pi^0) = 0.187 \pm 0.093_{internal} \pm 0.119_{external} = 0.19 \pm 0.15_{total},$$

where the errors, both internal and external, are much larger than for $f_P(f_2\pi^0/\rho\pi^0)$.

Combining the results for f_P from $f_2\pi^0/\rho\pi^0$, $K^+K^-/\pi^+\pi^-$, and $\rho\omega/\rho\pi^0$, we obtain an average value of $\overline{f_P} = 0.36 \pm 0.05$.

5 Summary

We have measured relative branching ratios for $\bar{\mathrm{p}}\mathrm{p}$ annihilation at rest. Results for the $\rho\pi^0$, $\rho\pi^0\pi^0$, $\rho\pi^0\pi^0\pi^0$, $\rho\omega$ and $f_2\pi^0$, $f_2\eta$ channels are given in Table 2. From the relative branching ratio $f_2\pi^0/\rho\pi^0$ the fraction of P-wave annihilation in a 16 bar gaseous hydrogen target is determined to be $f_P = 0.38 \pm 0.07$.

Acknowledgements

We would like to thank the CERN LEAR staff for their support and co-operation, and C. Amsler for helpful discussions.

This work was supported by the following institutions: the French CNRS/Institut National de Physique Nucléaire et de Physique des Particules, the French Commissariat à l'Energie Atomique, the Greek General Secretariat of Research and Technology, the Netherlands Foundation for Fundamental Research on Matter (FOM), the Portuguese JNICT and

INIC, the Ministry of Science and Technology of the Republic of Slovenia, the Swedish Natural Science Research Council, the Swiss National Science Foundation, the UK Science and Engineering Research Counsil (SERC), and the US National Science Foundation.

References

[1] S. Ahmad et al. (ASTERIX Collab.), Nucl. Instrum. Methods **A286** (1990) 76.

[2] E. Aker et al. (Crystal Barrel Collab.), Nucl. Instrum. Methods **A321** (1992) 69.

[3] A. Adamo et al. (OBELIX Collab.), Sov. J. Nucl. Phys. **55** (1992) 1732.

[4] R. Armenteros and B. French, in High Energy Physics, ed. E.H.S. Burhop, Vol. **4** (Academic Press, London, 1969) p. 237.

[5] C. Amsler and F. Myhrer, Annu. Rev. Nucl. Part. Sci. **41** (1991) 219.

[6] R. Adler et al. (CPLEAR Collab.), Phys. Lett. **286B** (1992) 180.

[7] Review of Particle Properties, Phys. Rev. **D45** (1992) part II.

[8] B. May et al. (ASTERIX Collab.), Phys. Lett. **225B** (1989) 450.

[9] R. Brun et al., CERN DD/EE/84-1 (1984).

[10] G. Backenstoss et al., Nucl. Phys. **B228** (1983) 424.

[11] C. Ghesquière, CERN-Collège de France, CERN Yellow Report 74-18 (1974) 436.

[12] C. Baltay et al., Phys. Rev. **145** (1966) 1103.

[13] M. Chiba et al., Phys. Rev. **D38** (1988) 2021; **D39** (1989) 3227.

[14] M. Foster et al., CERN-Collège de France, Nucl. Phys. **B8** (1968) 174.

[15] L. Adiels et al., Z. Phys. **C42** (1989) 49.

[16] B. May et al. (ASTERIX Collab.), Z. Phys. **C46** (1990) 191; Z. Phys. **C46** (1990) 203.

[17] P. Weidenauer et al. (ASTERIX Collab.), Z. Phys. **C47** (1990) 353.

[18] B. Schmid (Crystal Barrel Collab.), Ph.D. Thesis, Zürich 1991, unpublished.

[19] P. Weidenauer et al. (ASTERIX Collab.), Z. Phys. **C59** (1993) 387.

[20] R. Bizzarri et al., CERN-Collège de France, Nucl. Phys. **B14** (1969) 169.

[21] T.B. Day, G.A. Snow, and J. Sucher, Phys. Rev. Lett. **3** (1959) 61; Phys. Rev. **118** (1960) 864.

[22] L. Adiels et al., Z. Phys. **C35** (1987) 15.

[23] C. Amsler et al. (Crystal Barrel Collab.), Phys. Lett. **297B** (1992) 214.

[24] G. Reifenröther and E. Klempt, Nucl. Phys. **A503** (1989) 885; Phys. Lett. **245B** (1990) 129.

[25] M. Doser et al. (ASTERIX Collab.), Nucl. Phys. **A486** (1988) 493.

[26] C. Amsler, Private communication.

[27] R. Adler et al. (CPLEAR Collab.), Phys. Lett. **267B** (1991) 154.

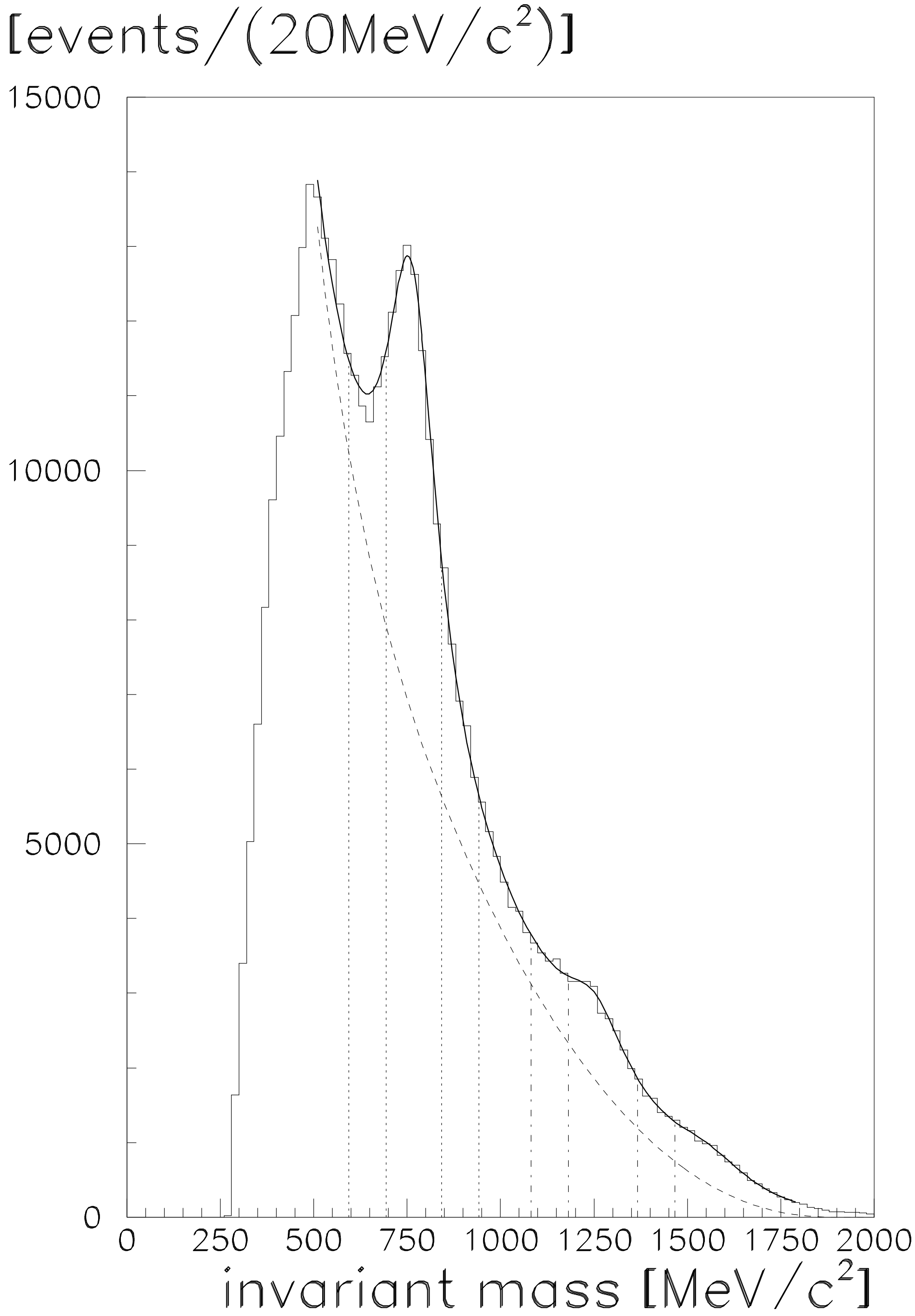

Figure 1: The invariant mass ($m_{\pi\pi}$) spectrum for final states with two charged particles of opposite sign, assumed to be pions. The spectrum was fitted to three Breit-Wigner functions, plus a background, parametrized as $F(m) = (p_5 - m)^{p_1} e^{p_2} + (p_5 - m)^{p_3} e^{p_4}$, where $m \equiv m_{\pi\pi}$. The central value, the width and the relative weight of each resonance were kept free, as well as the background parameters p_1 to p_5. The full line is the result of the fit, and the dashed line is the background contribution. The dotted (dash-dotted) lines delimit the slices used for the analysis of the ρ (f_2) momentum spectrum.

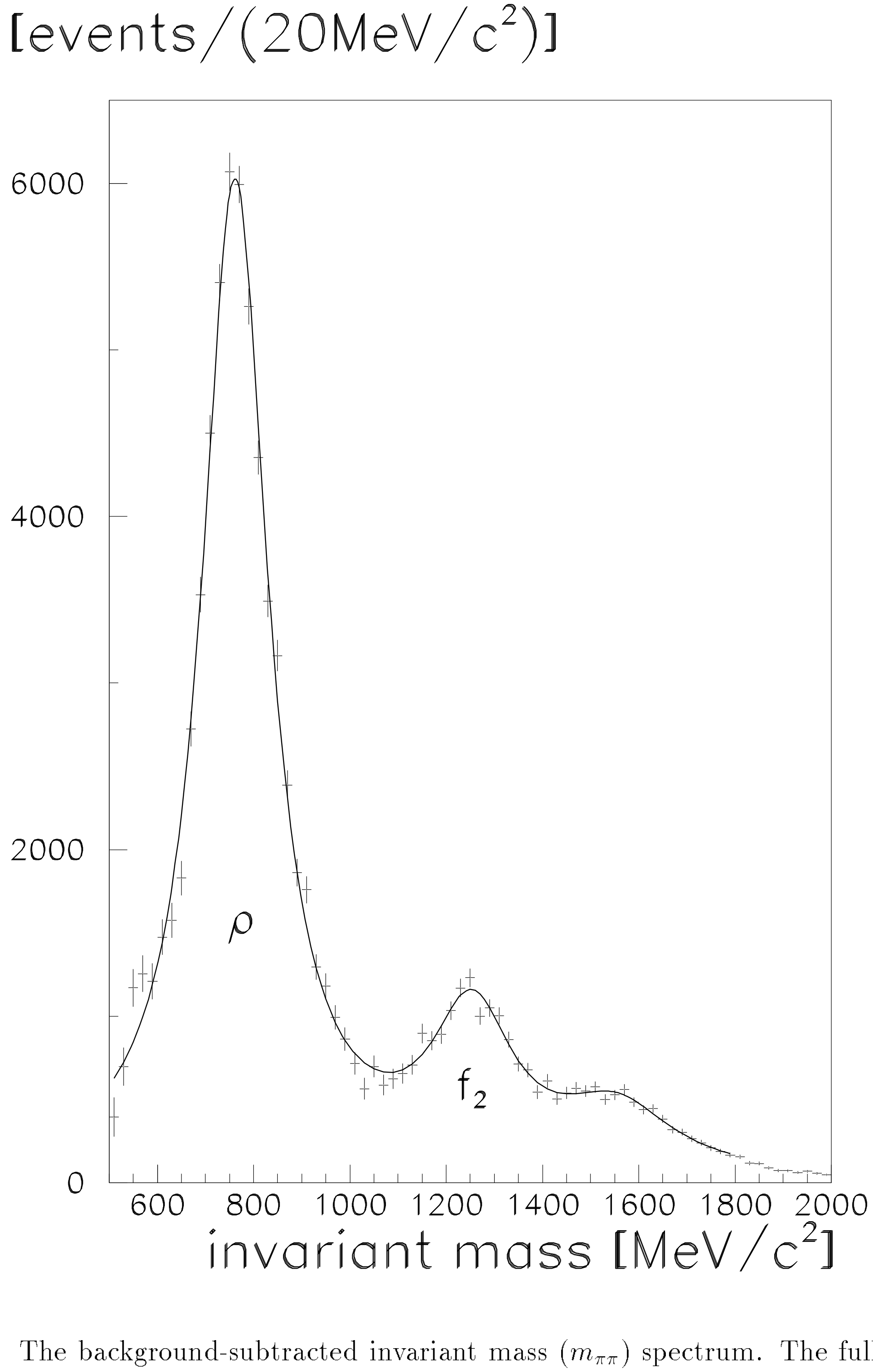

Figure 2: The background-subtracted invariant mass ($m_{\pi\pi}$) spectrum. The full line is the result, after background subtraction, of the fit described in Fig. 1.

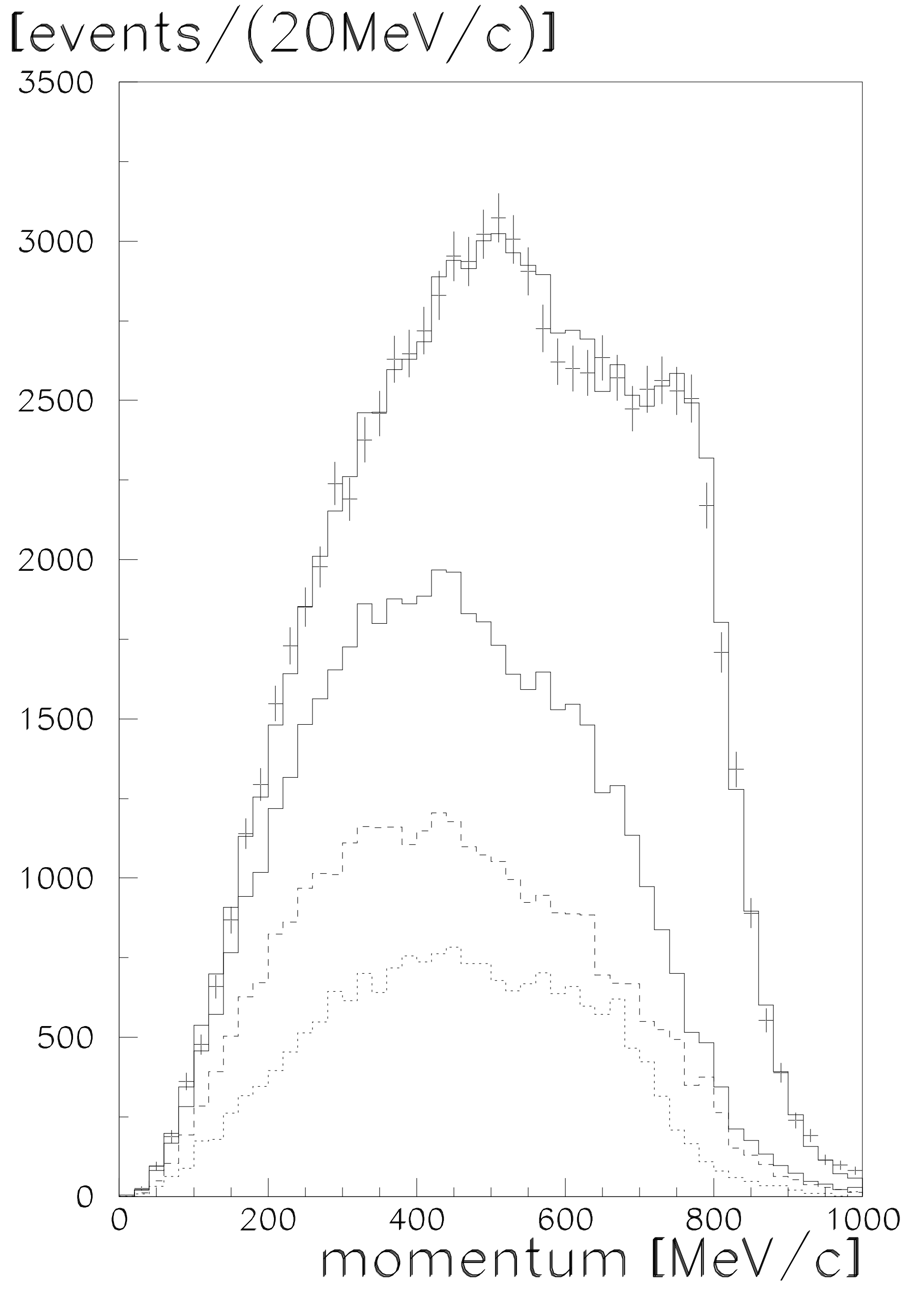

Figure 3: The momentum spectrum of the ρ slice as defined in Fig. 1. The dashed (dotted) line is the background from the low-mass (high-mass) slice, shown in Fig. 1 at the left (right) of the ρ-resonance slice. The ρ spectrum was fitted to the sum of the contributions from the various channels (computed by MC simulations and shown in Fig. 4), plus the background. The relative weights of these slices, and of each of the MC-generated contributions, were kept free in the fit. The upper full line is the result of the fit, and the lower full line represents the total background.

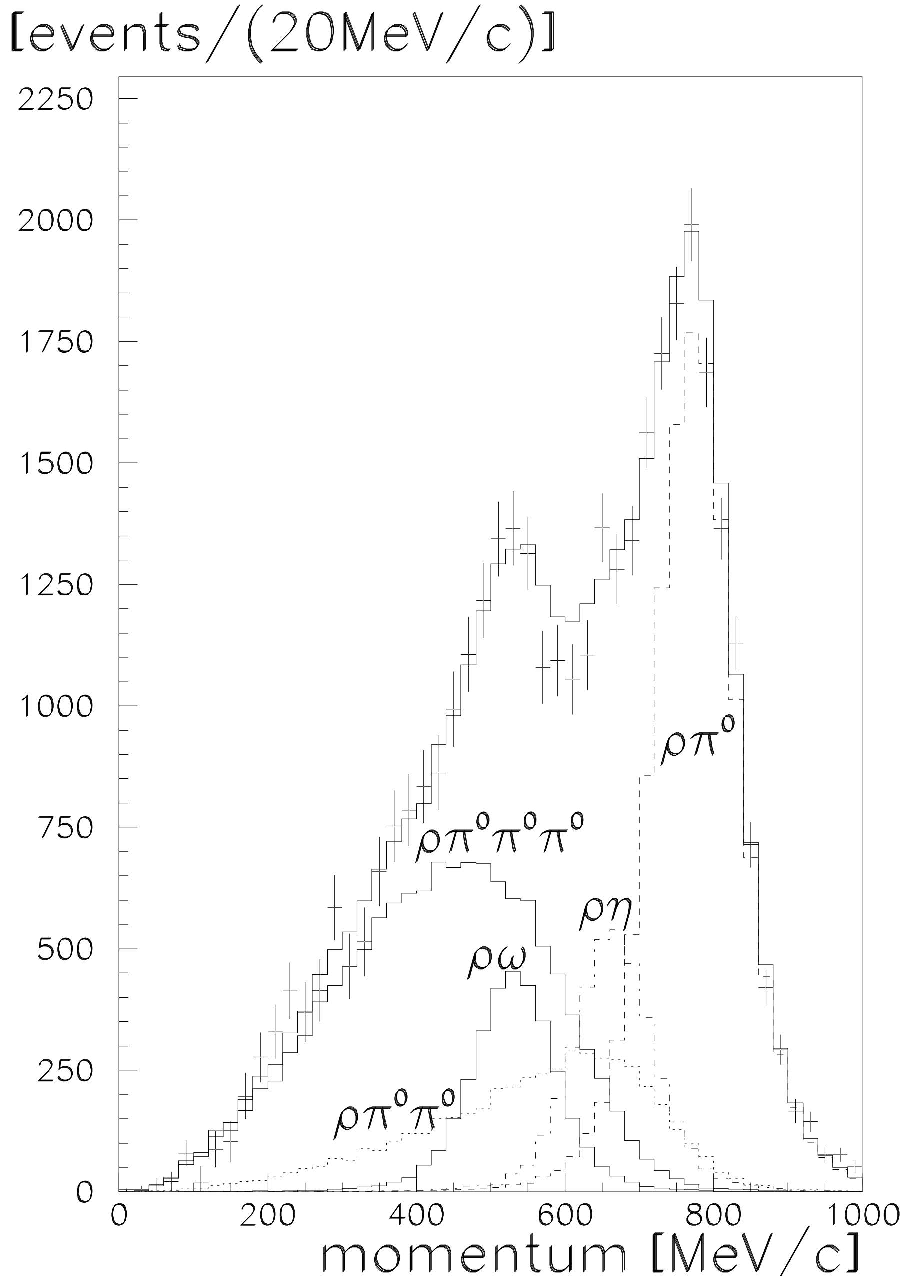

Figure 4: The momentum spectrum of the ρ slice after background subtraction, and the fitted MC-generated distributions for the individual channels used in the fit.

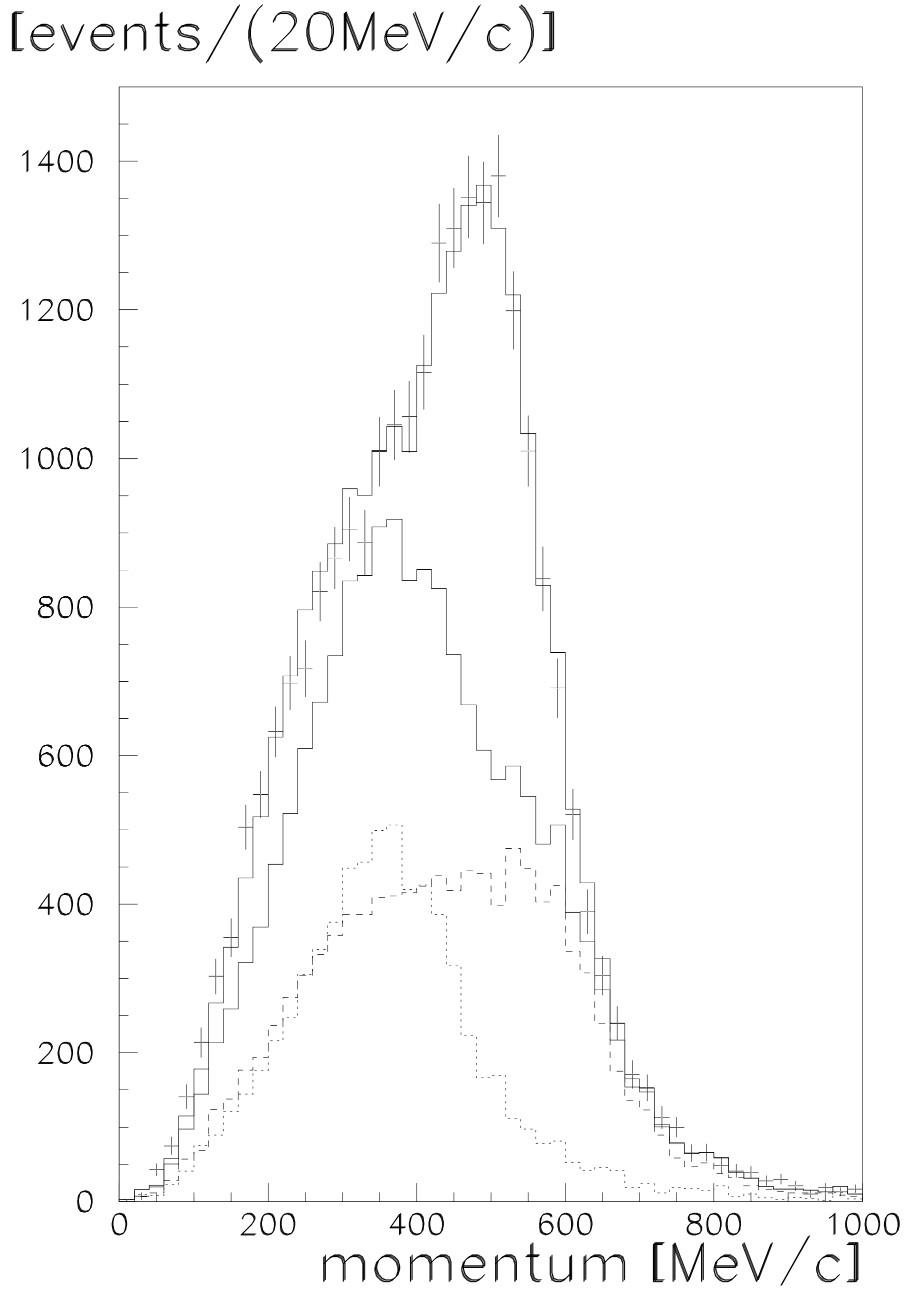

Figure 5: The momentum spectrum of the f_2 slice as defined in Fig. 1. The dashed (dotted) line is the background from the low-mass (high-mass) slice, shown in Fig. 1 at the left (right) of the f_2-resonance slice. The f_2 spectrum was fitted to the sum of the contributions from the various channels (computed by MC simulations and shown in Fig. 6), plus the background. The relative weights of these slices, and of each of the MC-generated contributions, were kept free in the fit. The upper full line is the result of the fit, and the lower full line represents the total background.

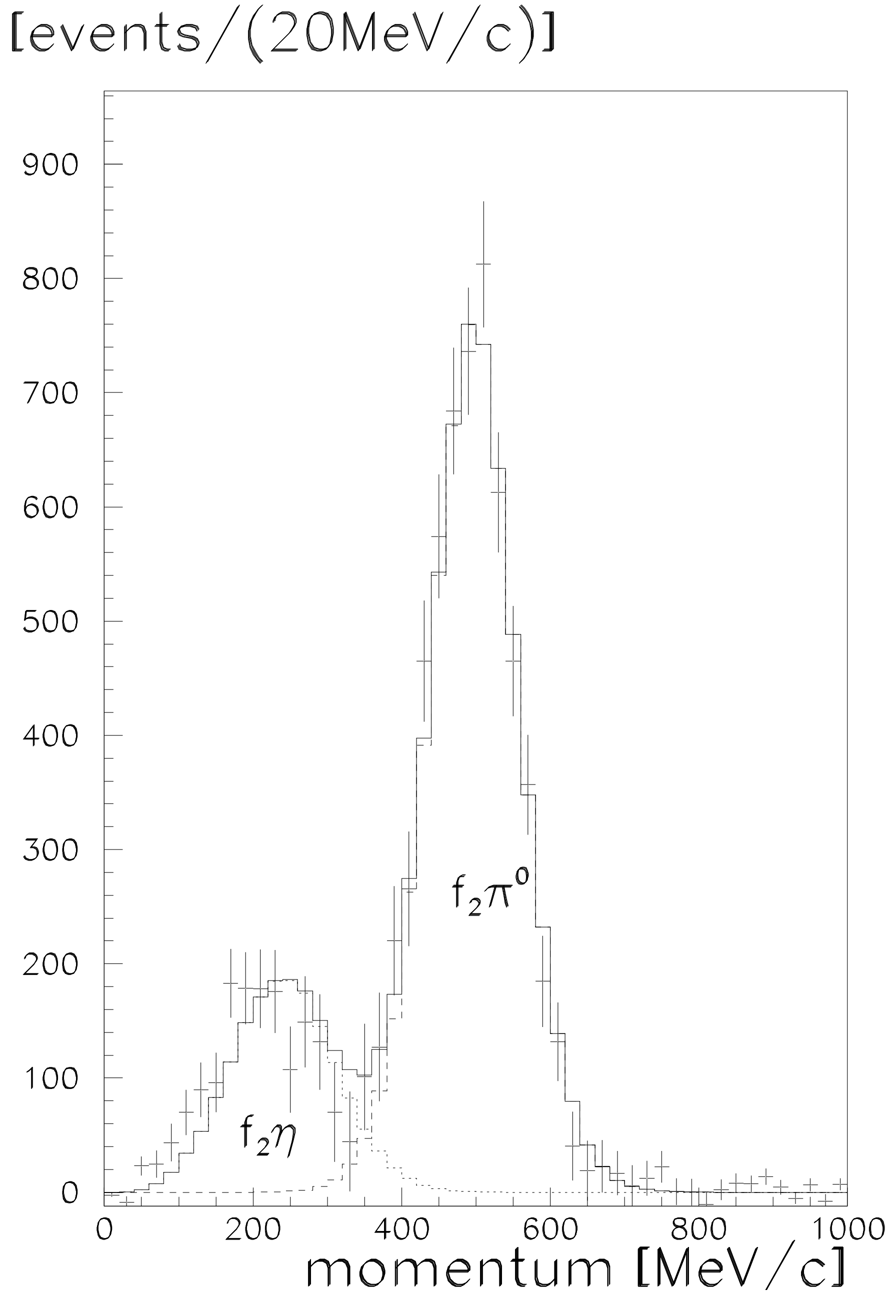

Figure 6: The momentum spectrum of the f_2 slice after background subtraction, and the fitted MC-generated distributions for the two channels used in the fit.